Kinetic Analysis of the L-Ornithine Transcarbamoylase from *Pseudomonas savastanoi* pv. phaseolicola That Is Resistant to the Transition State Analogue (*R*)-N^{δ}-(*N*′-Sulfodiaminophosphinyl)-L-ornithine†

Matthew D. Templeton,*,‡ Laurie A. Reinhardt,§ Charles A. Collyer,|| Robin E. Mitchell,‡ and W. Wallace Cleland§

Horticulture and Food Research Institute of New Zealand, Mt. Albert Research Centre, Auckland, New Zealand, Institute for Enzyme Research and Department of Biochemistry, University of Wisconsin, Madison, Wisconsin 53726, and School of Molecular and Microbial Biosciences, Sydney University, Sydney 2006, Australia

Received December 7, 2004; Revised Manuscript Received January 19, 2005

ABSTRACT: (*R*)-N^{δ}-(*N*′-Sulfodiaminophosphinyl)-L-ornithine (PSorn) is the active component of a phytotoxin, called phaseolotoxin, produced by *Pseudomonas savastanoi* pv. phaseolicola. PSorn acts as a potent transition state (TS) inhibitor of ornithine transcarbamoylase (OTCase, E.C. 2.1.3.3) that binds to the OTCase from *Escherichia coli* (ARGI) with a dissociation constant of 1.6 pM. While inhibition of OTCase can lead to arginine auxotrophy, *P. savastanoi* pv. phaseolicola is able to synthesize toxin while growing on minimal medium. This is achieved by the expression during toxin production of a second gene encoding OTCase activity that is not inhibited by PSorn (ROTCase). ROTCase is orthologous to other OTCases, but it has substitutions to key conserved amino acids, particularly to those around the carbamoyl phosphate (CP) binding site and in the ornithine binding "SMG" loop. This suggests that the topology of the CP binding site and the closure of the SMG loop may be different in ROTCase. Steady-state kinetics indicate that ROTCase has an ordered mechanism, and the ^{13}C kinetic isotope effect (IE) in CP indicates that it is the first substrate to bind. However, unlike other OTCases, there is a random element to the mechanism since the second substrate ornithine (Orn) was unable to completely suppress the IE to unity. The most striking difference with ROTCase is the reduction of k_{cat} to between 1% and 2% of other OTCases. This is consistent with the large IE that ROTCase exhibits (3.4%) at near-zero Orn. These results suggest that the chemistry of the reaction is rate limiting for ROTCase. ROTCase has a substrate and inhibitor profile similar to that of other OTCases. The CP binding affinity of ROTCase is diminished when compared with that observed from ARGI, and inhibitors that compete with the CP binding site have K_i values at least 10-fold higher for ROTCase than for ARGI. Arsenate did not inhibit ROTCase, and bisubstrate and dead-end inhibitors are less effective inhibitors of ROTCase than ARGI. These data suggest that PSorn is unable to bind tightly to either the apo or activated forms of ROTCase at the expense of CP binding and reduced k_{cat}.

Pseudomonas savastanoi pv. phaseolicola (synonym *Pseudomonas syringae* pv. phaseolicola) causes halo blight of French beans (*Phaseolus vulgaris* L.). The disease symptoms include chlorosis around the site of infection that is caused by the diffusion of a toxin named phaseolotoxin. Phaseolotoxin has a highly unusual structure consisting of a tripeptide backbone of L-homoarginine, L-alanine, and L-ornithine (Orn),[1] and attached to the δ-amino group of Orn is an (*R*)-sulfodiaminophosphinyl residue (Figure 1a) (*1*, *2*). In plants, the tripeptide is cleaved by peptidases to release (*R*)-N^{δ}-(*N*′-sulfodiaminophosphinyl)-L-ornithine (PSorn); it is the most active component of the toxin (*3*) (Figure 1b). PSorn has been shown to be a potent active site directed inhibitor of the enzyme ornithine transcarbamoylase (OTCase; E.C. 2.1.3.3) which binds to the enzyme from *Escherichia coli* ARGI, with a dissociation constant of 1.6 pM (*4*). OTCase catalyzes the condensation of carbamoyl phosphate (CP) and Orn to form L-citrulline and inorganic phosphate. In plants and microbes it is involved in arginine biosynthesis, whereas in mammals it is the first step of the urea cycle. OTCase has an ordered bi-bi mechanism where

† This research was supported by the Marsden Fund, Contract HRT801 to M.D.T. and R.E.M., and Grant GM 18938 from the National Institutes of Health to W.W.C.

* To whom correspondence should be addressed at HortResearch, Private Bag 92-169, Auckland, New Zealand. Phone: +64-9-815-4200 ext 7316. Fax: +64-9-815-4201. E-mail: mtempleton@hortresearch.co.nz.

‡ Mt. Albert Research Centre.

§ University of Wisconsin.

|| Sydney University.

[1] Abbreviations: ARGI, ornithine transcarbamoylase encoded by the *Escherichia coli argI* gene; AVA, 5-aminovaleric acid; C_f, forward commitment to catalysis; CP, carbamoyl phosphate; DAB, diaminobutane; DABA, diaminobutyric acid; DTT, dithiothreitol; EDTA, ethylenediaminetetraacetic acid; ESMS, electrospray mass spectrometry; IE, isotope effect; IPTG, isopropyl β-D-thiogalactopyranoside; NAC, near attack conformers; Orn, L-ornithine; OTCase, ornithine transcarbamoylase; PALO, *N*-(phosphonoacetyl)-L-ornithine; PCR, polymerase chain reaction; PMSF, phenylmethanesulfonyl fluoride; PSorn, (*R*)-N^{δ}-(*N*′-sulfodiaminophosphinyl)-L-ornithine; ROTCase, OTCase encoded by *argK* resistant to PSorn; SDS−PAGE, sodium dodecyl sulfate−polyacrylamide gel electrophoresis; TAPS, *N*-tris(hydroxymethyl)methyl-3-aminopropanesulfonic acid; Tris, tris(hydroxymethyl)-aminomethane; TS, transition state.

10.1021/bi047432x CCC: $30.25
Published on Web 02/19/2005

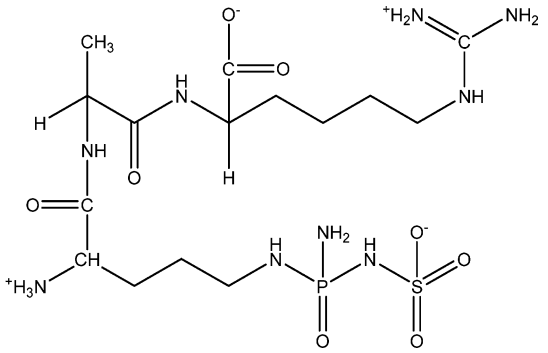

(a) Phaseolotoxin: (*R*)-N^{δ}-(*N'*-sulfodiamino-phosphinyl)-L-ornithinyl-L-alanyl-L-homoarginine.

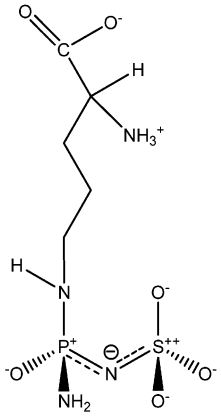

(b) PSorn: (*R*)-N^{δ}-(*N'*-sulfodiaminophosphinyl)-L-ornithine.

FIGURE 1: Structures of phaseolotoxin and PSorn. (a) Structure of phaseolotoxin (*2*). (b) Structure of PSorn bound to the OTCase active site deduced from crystal structure data and quantum mechanics (*4*, *20*).

CP is the first substrate to bind, leading to a conformational change that allows Orn to bind and catalysis to occur (*5*, *6*). A detailed kinetic analysis of the OTCase from *E. coli* W revealed a Theorell−Chance mechanism where the concentration of the ternary complex is insignificant under steady-state conditions (*7*). The reaction mechanism involves nucleophilic attack of the δ-amino group of Orn on the carbonyl of CP. A detailed pH study suggested that only the zwitterion of Orn (with an unprotonated δ-amino group) is a substrate (*8*−*11*). Others have suggested that Cys303 may be involved in deprotonation of the Orn cation prior to nucleophilic attack (*12*). By analogy with aspartate transcarbamoylase it is envisaged that the OTCase reaction proceeds via a tetrahedral intermediate near the TS, which collapses following an intramolecular proton transfer from the δ-amino group of Orn to the phosphate (*13*, *14*).

A number of crystal structures of OTCases with substrates, substrate analogues, and inhibitors bound to the active site have now been solved (*4*, *12*, *15*−*19*). The structural data have largely confirmed previous differential spectroscopic and kinetic analysis that showed binding of the first substrate CP was followed by a global conformational change in the enzyme that enabled binding of Orn. The binary and ternary structures are very similar except for the position of the "SMG" loop (residues 225−246) which closes into the active site upon the binding of Orn (*15*). The crystal structure of the PSorn/OTCase complex revealed that the tetrahedral phosphinyl group of PSorn mimics the tetrahedral carbonyl of the TS (*4*). The X-ray structure also revealed that the nitrogen bridging the phosphinyl group and the sulfate is strongly hydrogen bonded to the ϵ nitrogen of Arg57 and is in a planar conformation. This indicated that it is the imino tautomer of PSorn which is bound at the active site (*4*). Analysis of the hydrogen bonding of the tetrahedral phosphinyl group to the enzyme indicated that the *R* isomer of PSorn is bound to the active site (*4*). A quantum chemical study of PSorn bound to Arg57 and Arg106 indicated that there was little π-delocalization and the bonds between oxygen and phosphorus or sulfur were single or semipolar (Figure 1b) (*20*).

The producing organism, *P. savastanoi* pv. phaseolicola, is capable of synthesizing phaseolotoxin when growing on minimal media, raising the question of how it is able to synthesize arginine. Assays of OTCase activity during phaseolotoxin biosynthesis indicated that *P. savastanoi* pv. phaseolicola possessed an OTCase activity that was not inhibited by either phaseolotoxin or PSorn (*21*, *22*). This was confirmed using molecular genetics which showed that *P. savastanoi* pv. phaseolicola possesses two genes which code for OTCase activity (*23*, *24*). The first of these, *argF*, is expressed under conditions where phaseolotoxin is not synthesized, such as growth at 28 °C. The predicted amino acid sequence and sensitivity to PSorn of *argF* are similar to those of other OTCases (*22*, *23*). The second gene encoding OTCase activity, *argK*, is expressed only during phaseolotoxin synthesis and resides on a 28 kb genomic DNA fragment which contains the phaseolotoxin biosynthetic genes (*25*−*27*). The predicted amino acid sequence of *argK* also has strong homology to other OTCases (30−49% identity), particularly to catabolic OTCases from bacteria (*23*, *24*). However, there are changes to otherwise conserved, key residues around the CP and Orn binding sites (*23*). The PSorn/OTCase structure suggests that the conserved residues altered in *argK* are not generally those whose side chains directly hydrogen bond with PSorn. The exception is Gln82, which is hydrogen-bonded to the sulfate and is an arginine in OTCase (Table 1). In addition, the sequence immediately after the SMG residues of the SMG loop differs from those conserved in other OTCases (Figure 2). An intriguing question is raised: if PSorn is a potent TS analogue, how does ROTCase catalyze the formation of citrulline?

Preliminary evidence suggests that *argK* encodes an OTCase activity that is not inhibited by PSorn (ROTCase); however, previous kinetic analysis of ROTCase was ambiguous. Jahn et al. (*28*) suggested there was little difference between the kinetic characteristics of the *argF* gene product and ROTCase activities from *P. savastanoi* pv. phaseolicola, whereas Templeton et al. (*29*) suggested ROTCase has an equilibrium-ordered mechanism and reduced affinity for CP compared to other OTCases. To carry out a more detailed kinetic analysis, we have expressed *argK* in *E. coli* and purified the recombinant gene product, ROTCase, to homogeneity. A detailed kinetic analysis of ROTCase has been performed using steady-state kinetics and IE. A comparison of the kinetic constants and mechanism of ROTCase with other OTCases is made, and the mechanism of resistance to PSorn is discussed.

Table 1: Structural and Functional Significance of Selected Amino Acids in *E. coli* OTCase and Their Unique Substitutions in ROTCase

CP binding site		
E. coli OTCase residue	substitution in ROTCase	function in *E. coli* OTCase
Glu52	Leu54	carboxylate group H-bonds to Gln82 from an adjacent subunit in the trimeric apo structure; note Gln82 is Arg in ROTCase and therefore this intersubunit H-bond does not exist in ROTCase
Thr56	Gly58	backbone amide H-bonds to sulfo group of PSorn
Arg59	Ser61	guanidinium ion forms a salt bridge with Glu64
Glu64	Val66	carboxylate forms a salt bridge with Arg59
Gln82	Arg84	side chain amide H-bonds to sulfo group of PSorn; introduction of a guanidinium ion in ROTCase will alter the electrostatics of the CP binding site

```
ROTCase 2° structure              ss sss                hh
ROTCase SMG loop sequence   225 ADV IYTDVWISMG ESVSV-EERI
Conserved amino acids          **  ****** *** *      ***
ARGI SMG loop sequence      225 ADF IYTDVWVSMG EAKEKWAERI
ARGI 2° structure                 ss sss           hhhhhhh
```

FIGURE 2: Comparison of the Orn binding site and the 225−246 SMG loop between ROTCase and ARGI. A lineup of residues 225−246 around the conserved Orn binding motif SMG loop (in blue). The unique -SVSV- sequence in ROTCase which is not conserved in other OTCases is highlighted in red. The secondary structure prediction for ROTCase was carried out using Jpred (*44*).

EXPERIMENTAL PROCEDURES

Materials. CP (disodium salt), DTT, EDTA, PMSF, ADP, TAPS, Orn, and carbamate kinase were from Sigma-Aldrich (Milwaukee, WI). AVA, DAB, and DABA were from ACROS Organics (Fischer Scientific, Loughborough, Leicestershire, U.K.). Phaseolotoxin was purified from *P. savastanoi* pv. phaseolicola ICMP 4419 (*1*). PSorn was prepared from purified phaseolotoxin by treatment with leucine aminopeptidase (Sigma-Aldrich) (*3*). Sodium [^{14}C]-bicarbonate was purchased from Amersham-Pharmacia Biotech (Buckinghamshire, U.K.). Restriction enzymes were obtained from Invitrogen (Carlsbad, CA). Long-template high-fidelity *Taq* polymerase was purchased from Roche Biochemicals (Basel, Switzerland). All other chemicals, of AnalR grade or better, were purchased from BDH (VWR International Ltd., Poole, Dorset, U.K.).

Cloning and Expression of argK. The enzyme ROTCase is encoded by *argK* in *P. savastanoi* pv. phaseolicola. Genomic DNA was isolated from *P. savastanoi* pv. phaseolicola by the method of Rudner et al. (*30*). Primers were designed to the 5′ and 3′ regions of *argK*, and *Eco*RI and *Hin*dIII restriction sites were included for directional cloning into the pKK223-3 expression vector polylinker (Amersham-Pharmacia Biotech). PCR was used to amplify *argK*, and the gene was first cloned into pGEM-T (Promega, Madison, WI) and sequenced to ensure no PCR errors had been generated. The *argK* insert was then cloned into pKK223-3 to generate pKKargK, and positive clones were transformed into the *E. coli* host TB-2 [*E. coli* K12: Δ(argI-pyrB1) argF$^-$] which lacks both endogenous OTCase-encoding genes (*31*). A second expression vector with a C-terminal 6× His tag linked by two serines was constructed in the same vector. Overnight cultures of pKKargK were used to inoculate 2 L flasks containing 250 mL of terrific broth to an OD_{550} of approximately 0.6. The flasks were incubated for a further 2−3 h. Although pKK223-3 contains the IPTG-inducible tac promoter (*32*), IPTG was not required for high level expression of ROTCase.

Purification of ROTCase. ROTCase was assayed as described in Langley et al. (*4*) using the colorimetric method of Boyde and Rahmatullah (*33*). *E. coli* TB-2 cells expressing ROTCase were resuspended in 50 mM TAPS, pH 8.0, containing 1 mM each of DTT, EDTA, and PMSF. The cells were disrupted with a sonicator (Dynatech, Farmingdale, NY) at 60% output for 5 min using the medium probe. The cell-free extract was brought to 40% saturation with $(NH_4)_2SO_4$ and the precipitate discarded. All chromatographic procedures were performed using an FPLC (Amersham-Pharmacia Biotech). The 40% $(NH_4)_2SO_4$ supernatant was chromatographed on a fast-flow phenyl-Sepharose (low substitution, 1.6 × 10 cm) column (Amersham-Pharmacia Biotech) with a linear gradient of 1.0−0 M $(NH_4)_2SO_4$ in 50 mM TAPS, pH 8.0. Positive fractions were brought to 60% saturation with $(NH_4)_2SO_4$, and the precipitate was resuspended and chromatographed on a Superdex 200 column (1.6 × 60 cm). ROTCase-containing fractions were buffer exchanged with 40 mM K_2HPO_4/citric acid, pH 4.0, and purified further on a SP-Sepharose column (5 mL) with a pH gradient of 4−6 in 40 mM K_2HPO_4/citric acid. ROTCase-positive fractions were desalted using a PD-10 (Amersham-Pharmacia Biotech) column equilibrated in 50 mM TAPS, pH 8.5, and frozen in 100 μL aliquots at −80 °C until use. ROTCase with a C-terminal 6× His tag was purified using Ni^{2+}-NTA His Bind resin (Novagen, Madison, WI). Resin (1−2 mL) was added to cell-free extracts prepared as described earlier and washed in buffer containing 50 mM imidazole and 1 M NaCl. ROTCase was eluted with 0.5 M imidazole, pH 8.0, desalted on a PD-10 column equilibrated in 50 mM TAPS, pH 8.5, and stored at −80 °C until required. Steady-state kinetics and IE were carried out with conventionally purified ROTCase while alternate substrate and inhibitor work was performed with His-tagged ROTCase.

OTCase from *E. coli* (encoded by *argI*) was purified using PALO affinity chromatography as described by Templeton et al. (*34*). SDS−PAGE was carried out using the Mini Protean II system from Bio-Rad. Electrospray mass spectrometry (ESMS) was performed using a Finnigan LC DECA (Thermo-Finnigan, San Jose, CA) instrument in the positive ion mode in 50% aqueous methanol containing 1% formic acid. N-Terminal sequencing was carried out by the Protein Microchemistry Facility at Otago University, Dunedin, New Zealand.

Steady-State Kinetics. ROTCase has a pH optimum of 8.5 as determined using the tribuffer system of Ellis and Morrison (*35*). ROTCase was routinely assayed at 37 °C in 50 mM TAPS, pH 8.5. Initial velocities were measured in 1 mL with varying concentrations of CP (2, 4, 6, 8, and 10 mM) and Orn (0.125, 0.25, 0.375, 0.5, 1.0, and 1.5 mM)

and 0.6 pmol of enzyme. Samples (100 μL) were removed at 2, 4, 6, 8, and 10 min and quenched directly into color reagent (1 mL) (*33*). Reaction rates were linear over this time course, and initial velocities were calculated using ORIGIN (OriginLab, Northampton, MA). Initial velocities were analyzed and kinetic constants calculated using the programs described by Cleland (*36*). Fixed-time (10 min) assays for inhibitor and alternate substrate studies were performed at 37 °C in 100 μL of 50 mM TAPS, pH 8.5, with varying concentrations of substrates and inhibitors. Michaelis and inhibition constants were calculated from the secondary plots derived from double reciprocal plots using ORIGIN. Inhibitors that compete with the CP binding site were assayed with 3 mM Orn, 0.25, 0.5, 0.75 1.0, and 2 mM CP, and 1.0, 2.0, 5.0, 7.5, and 10 mM inhibitor. Alternate substrates for Orn were assayed at 10, 20, 30, 40, and 50 mM and at constant CP (5 mM). Inhibitors that compete with the Orn binding site were assayed at 0.25, 0.5, 1.0, and 2 mM concentrations of Orn and 0.1−10 mM inhibitor. The reverse reaction was assayed using either the phosphorolysis of citrulline, coupled with carbamate kinase, or the arsenolysis of citrulline (*7*, *37*). Activity was determined by assaying the disappearance of citrulline (*33*).

Substrate Specificity of ROTCase. The reaction of ^{14}C-CP with Orn and alternate substrates was carried out essentially as described by Marshall and Cohen (*38*). ^{14}C-CP was synthesized enzymatically in situ in a 1 mL reaction containing 200 mM NH_4Cl, pH 8.4, 40 mM $KHCO_3$, 5 units of carbamate kinase, 5 mM ATP, 10 mM $MgCl_2$, 50 mM potential alternate substrate, and either ARGI (100 units) or ROTCase (10 units). The reaction was incubated at 37 °C for 2 h and quenched with 100 μL of 10 M H_2SO_4. The quenched reaction was incubated at 37 °C for a further 2 h to ensure complete decomposition of CP. Unincorporated $^{14}CO_2$ was removed by bubbling CO_2 gas through the reaction for 10 min. Counts in the remaining solution were measured in a LKB 1214 Rackbeta scintillation counter.

^{13}C Isotope Effects on the ROTCase-Catalyzed Reaction. The heavy atom ^{13}C IEs in CP in the ROTCase-catalyzed reaction were analyzed as for aspartate transcarbamoylase (*39*) by measuring the $^{13}C/^{12}C$ ratio of CO_2 derived from CP using the internal competition method. The ratio of $^{13}C/^{12}C$ of the residual CP present in ROTCase-catalyzed reactions that were allowed to react only partially was compared to the ratio of unreacted CP determined by acid hydrolysis. The ^{13}C isotope effect was measured over a range (0−100 mM) of Orn concentrations. The reactions were run under N_2 gas, which was passed through an ascarite column to remove CO_2, and an acidic water solution to prevent water loss from the reactions. Solutions of 50 mM TAPS, 0.2 mM EDTA, 2 mM DTT, pH 6, and 0.05−0.1 M Orn in 50 mM TAPS, 0.2 mM EDTA, and 2 mM DTT were sparged for 1.5 h and then brought to pH 8.5 with CO_2-free 10 M NaOH. A solution of 0.13−0.18 M CP on ice was sparged for 1 h. Buffer (5−8 mL), CP (1.0−1.2 mL), and enzyme were syringed into closed reaction flasks equipped with a sidearm stopcock and septum. Orn was added to attain the desired concentration to start the reaction. As the reaction proceeded, additional Orn was added dropwise to keep the concentration constant using the experimental rate of the enzyme reaction to determine the rate of addition. The reactions had proceeded from 6% to 57% before being quenched after 15 min with 0.5 mL of H_2SO_4. The residual CP was allowed to completely decompose to CO_2, NH_4^+, and inorganic phosphate at 37 °C for 2 h. The CO_2 was distilled through two dry ice/2-propanol traps and isolated on a high vacuum line. The gas was analyzed on a Finnigan MAT Delta E isotope ratio mass spectrometer (Thermo Finnigan). The $^{13}C/^{12}C$ ratio of unreacted CP was determined using the same method, except no Orn or enzyme was added. Buffer samples of Orn and enzyme without CP subjected to this method did not produce CO_2. Also, a solution of only CP and buffer without addition of H_2SO_4 and heating did not produce CO_2.

The fraction of reaction was calculated from the amount of citrulline produced, determined colorimetrically (*33*), and the amount of CO_2 produced, measured manometrically.

The ^{13}C IE or $^{13}(V/K)$ was determined using the formula:

$$^{13}\left(\frac{V}{K}\right) = \frac{\log(1-f)}{\log\left[(1-f)\left(\frac{R_s}{R_o}\right)\right]} \quad (1)$$

where f is fraction of reaction, R_s is the $^{13}C/^{12}C$ of residual CP determined from partial ROTCase-catalyzed reactions, and R_o is the $^{13}C/^{12}C$ ratio of unreacted CP. The ^{13}C isotope effect versus concentration was fitted to the following equation for a hyperbola:

$$y = A\left(1 + \frac{x}{K_{in}}\right)\Big/\left(1 + \frac{x}{K_{id}}\right) \quad (2)$$

where y is the observed ^{13}C IE, x is the final Orn concentration, A is the isotope effect at an Orn concentration extrapolated to zero, K_{id} is the Orn concentration that half-suppresses the isotope effect, and the quantity $(A)(K_{id})/K_{in}$, the asymptote, is the isotope effect at infinite concentration of Orn.

RESULTS

Expression and Purification of ROTCase. ROTCase did not bind to the PALO affinity column which has been used successfully to purify OTCases from other sources (*34*, *40*). Initially, ROTCase was purified in a three-step chromatographic procedure as described in the Experimental Procedures section. The identity of the final ROTCase preparation was confirmed by ESMS (observed mass 36562.0 Da). This corresponds to the predicted mass of 36561.68 Da per subunit with the N-terminal start methionine present. This was confirmed using N-terminal sequencing [in contrast, the start methionine on ARGI is cleaved (*4*)]. Significant ROTCase activity was lost during purification despite the use of additional protease inhibitors, dead-end inhibitors, substrates, products, or glycerol. To overcome this problem, ROTCase was fused with a C-terminal 6× His tag linked by an additional two serine residues. An N-terminal 6× His tag did not express active enzyme, and a C-terminal tag without the linker did not bind to the Ni^{2+} column. Using the C-terminal His tag ROTCase was purified to ∼95% homogeneity using Ni^{2+} affinity chromatography in a single step. The observed mass by ESMS was 37559 Da (predicted 37556.8 Da). ROTCase purified by either method had a final specific activity of between 37 and 54 units/mg of protein. The elution volume from the Superdex 200 FPLC column

Table 2: Kinetic Constants from ROTCase and ARGI[a]

kinetic parameter	ROTCase	ARGI
k_{cat} (s^{-1})	49 ± 3	3450
K_{CP} (mM)	0.09 ± 0.04	0.24
K_{iCP} (mM)	0.151 ± 0.025	0.013
K_{orn} (mM)	1.1 ± 0.1	0.86
K_{iorn} (mM)	1.9 ± 1.1	0.047
mid isotope point[b] (mM)	1.7 ± 0.4	ND[c]

[a] OTCase assays were carried out at 37 °C in 50 mM TAPS−NaOH, pH 8.5, as described in the Experimental Procedures. The rate equation fitted was $\log v = \log[VAB/(K_{ia}K_b + K_aB + K_bA + AB)]$, where *A* and *B* are CP and Orn concentrations. [b] Level of Orn that reduced the IE halfway from its value at near zero Orn to the value at infinite Orn; this should equal K_{iorn}. [c] Not determined.

of ROTCase is the same as OTCase from *E. coli*, which suggests that the enzyme is a trimer.

Steady-State Kinetics. The initial velocities generated under steady-state conditions were fitted to the rate equations for a sequential and an equilibrium-ordered mechanism. The program that gave the best fit of the data was SEQUENL ($\log v = \log[VAB/(K_{ia}K_b + K_aB + K_bA + AB)]$), based on the data giving the lowest σ value and the most even distribution of errors. This indicates that ROTCase has a sequential mechanism, as has been observed for all OTCases studied thus far. The derived kinetic constants for ROTCase and those for ARGI are shown in Table 2. The steady-state kinetic constants for ARGI were determined using the same buffer, pH, and temperature that were used for ROTCase to enable a direct comparison between the two enzymes. The kinetic constants calculated for ARGI broadly agree with those determined previously for *E. coli* OTCases (*7*, *8*, *11*). ROTCase has a 10-fold higher K_{iCP} and a 2.5-fold lower K_{CP} than ARGI. The most striking difference between the two enzymes is that ROTCase has a much reduced turnover number of 49 s^{-1} compared with 3450 s^{-1} for ARGI. ROTCase is less catalytically efficient than ARGI. The K_{orn}, however, is similar to those found for other OTCases.

Kinetic Isotope Effects. To determine the substrate binding order of ROTCase, the kinetic IE was determined. ^{13}C IEs on the ROTC-catalyzed reaction were measured at pH 8.5 by isotopic analysis ($^{13}C/^{12}C$) of CO_2 derived from CP (Figure 3). For a bisubstrate enzymatic reaction, the dependence of the IE for one substrate on the concentration of the other substrate is indicative of the enzyme's kinetic mechanism. The graph clearly shows that the observed ^{13}C IE has a large dependence on the concentration of the second substrate Orn (0−100 mM). The hyperbolic relationship indicated a largely ordered mechanism with CP binding prior to Orn. The data were fitted to eq 2, and the hyperbola shown is the calculated fit. At high concentrations of Orn the observed isotope effect is at its minimum (1.012 ± 0.001). Although reduced, at high concentrations of Orn, the observed isotope ratio does not go to unity. This indicates that the commitments to reaction are increasing as the concentration increases but do not completely mask the isotope effect. Thus while the mechanism is largely ordered, there is some random binding of substrates (Scheme 1).

The calculated Orn concentration for which the observed isotope effect is suppressed halfway, K_{iorn}, is 1.7 ± 0.4 mM. This value agrees well with the 1.9 ± 1.1 mM calculated from the steady-state kinetic data (Table 2). At low concentrations of Orn, the isotope effect is at its maximum (1.034 ± 0.001). The size of the maximum suggests that the chemical step producing this ^{13}C IE is significantly rate determining.

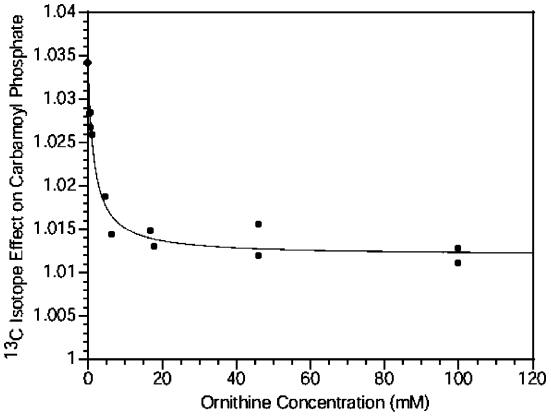

FIGURE 3: ^{13}C IE on CP for the ROTC-catalyzed reaction measured at pH 8.5 with saturating levels of CP at varying concentrations of Orn (mM). The effects were measured in 50 mM TAPS, 0.2 mM EDTA, and 2 mM DTT at 24 °C. The experimental data (●) were fitted to eq 2 (—). The maximum ^{13}C IE, 1.034 ± 0.001, was determined by extrapolation to 0 mM Orn. The ^{13}C IE at infinity is 1.012 ± 0.001. The concentration of Orn that half-suppresses the ^{13}C IE is 1.7 ± 0.4 mM.

Scheme 1

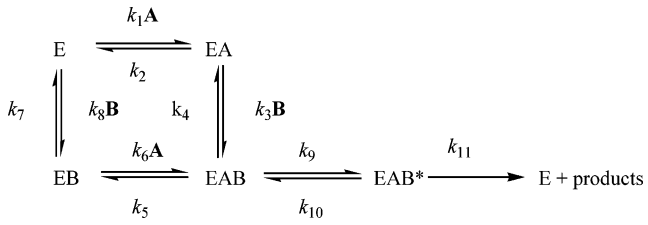

If the intrinsic ^{13}C isotope effect is assumed to be 1.039 (the value for ATCase with the asparate analogue L-cysteine sulfinate) (*39*), then the commitment in the forward direction (C_f) can be calculated from

$$^{13}\left(\frac{V}{K}\right)_{obs} = \frac{1.039 + C_f}{1 + C_f} \quad (3)$$

At low concentrations of Orn, the observed value of 1.034 gives a C_f of 0.147. In Scheme 1 at low concentrations of Orn

$$C_f = (k_{11}/k_{10})[1 + k_9/(k_4 + k_5)] \quad (4)$$

or since Orn is probably not sticky and $k_4 \gg k_9$

$$C_f = k_{11}/k_{10} = 0.147 \quad (5)$$

At high concentrations of Orn, the observed value of 1.012 gives a C_f value of 2.25. At high concentrations of Orn

$$C_f = (k_{11}/k_{10})(1 + k_9/k_5) \quad (6)$$

Substituting the values for C_f and k_{11}/k_{10} gives $k_9/k_5 = 14.3$. The ratio of the off rate for CP from the ternary complex to the net rate constant for conversion of the ternary complex to products is

$$k_5/[k_9k_{11}/(k_{10} + k_{11})] = (k_5/k_9)(1 + k_{10}/k_{11}) = 0.55 \quad (7)$$

Table 3: Kinetic Constants from ROTCase and ARGI for Inhibitors and Alternate Substrates

	ROTCase		ARGI	
	inhibition	K_i (mM)	inhibition	K_i
vary CP				
PSorn	no inhibition up to 30 μM		TS analogue	1.6 pM[a]
PALO	not determined		bisubstrate inhibitor	770 nM[b]
phosphate	competitive inhibitor	3.8	competitive inhibitor	2.0 mM
arsenate	no inhibition up to 10 mM		competitive inhibitor	5.0 mM

	ROTCase			ARGI		
	substrate/inhibitor	K_m or K_i (mM)	k_{cat} (s^{-1})	substrate/inhibitor	K_m or K_i (mM)	k_{cat} (s^{-1})
vary Orn						
L-lysine	substrate	25	0.0036	substrate	20.4	1.3
5-aminovaleric acid	neither substrate nor inhibitor			neither substrate nor inhibitor		
diaminobutane	substrate	43.5	0.025	substrate	24	0.38
diaminobutyric acid	inhibitor	1.1		inhibitor	6.4	
norvaline	inhibitor	1.7		inhibitor	0.16	
reverse reaction (with arsenate)	not detectable			yes		
reverse reaction (with phosphate)	not detectable			yes		

[a] Langley et al. (*4*). [b] Penninckx and Gigot (*45*).

Thus CP is released from the ternary complex at just over half of the rate of the overall reaction.

These isotope effects can be compared to those obtained from OTCase from *E. coli* (*41*). The same dependence of ^{13}C IE on Orn concentration was found, but the maximum isotope effect determined was only 1.0095 ± 0.0007. In this case, the asymptote does go to unity at high concentrations of Orn. This difference in isotope effect can be explained by the much smaller turnover number (1.4%) determined for ROTCase as compared to ARGI. The chemical steps have become rate determining at nearly zero Orn levels for the ROTCase reaction, eliminating any commitments to catalysis. The value of 3.4% is close to the intrinsic isotope effect for this reaction. The isotope effects for ARGI were also previously determined using lysine, a slow substrate, instead of Orn (*41*). In this case an extremely high isotope effect (1.076) was found, showing that the chemical steps had become rate limiting.

Inhibitors and Alternate Substrates of ROTCase. A number of alternate substrates and inhibitors of OTCase were tested on ROTCase (Table 3). Inhibitors of OTCases which bind to the CP binding site have K_i values ~10-fold higher in ROTCase, except for arsenate which does not inhibit ROTCase up to 10 mM. PSorn did not inhibit ROTCase up to 30 μM (>10^6 × the K_i for ARGI inhibition).

Alternate second substrates lysine and diaminobutane were substrates for both ROTCase and ARGI with k_{cat} values 3−4 orders of magnitude lower for ROTCase than ARGI for Orn and K_m values 20−40-fold higher. AVA is neither a substrate nor inhibitor of either enzyme. This suggests that an α-amino group is required for substrate binding. Diaminobutyric acid and norvaline are inhibitors of both enzymes; however, they differ in their potency. Both compounds form a dead-end complex with either CP or phosphate. Norvaline is a weaker inhibitor of ROTCase compared to ARGI by an order of magnitude, while diaminobutyric acid is a stronger inhibitor relative to ARGI (Table 3).

Although the equilibrium for this reaction lies overwhelmingly in the forward direction, the reverse reaction can be assayed in vitro if the CP formed is removed either enzymatically with carbamate kinase or through rapid decomposition of carbamoyl arsenate (*37*). ROTCase did not catalyze the reverse reaction under either of these assay conditions, whereas the reverse reaction with ARGI was easily detected (Table 3).

DISCUSSION

PSorn is an exceptionally potent TS inhibitor of OTCases with a binding constant of 1.6 pM calculated for the enzyme from *E. coli* and has been shown to inhibit OTCase from all sources tested to date (*4*, *21*). An exception is the ROTCase activity encoded by the *argK* gene expressed in isolates of *P. savastanoi* pv. phaseolicola that produce phaseolotoxin (*21*, *22*, *29*). ROTCase has 30−49% amino acid sequence identity to other OTCases but differs in two key conserved motifs (*23*, *24*). The CP binding domain, in particular the STRTR CP binding motif, is SGRTS in ROTCase. In addition, the sequences following the SMG residues in the SMG loop are different (Figure 2). Of the many residues whose side chains form hydrogen bonds to PSorn in the complex with OTCase from *E. coli*, only one, Gln82, is altered (to arginine) in ROTCase. While the side chain of this arginine, Arg84 in ROTCase, may also function to bind the phosphate group of CP, this and other changes to the binding site are sufficient to predict a small but significant difference in the physical and electrostatic topology of the CP binding domain.

These predicted changes are reflected in both the steady-state kinetics and IE of ROTCase. Both of these techniques have given consistent results, which show that ROTCase retains a largely ordered mechanism with CP being the first substrate to bind, although there is a random element to the mechanism not observed in other OTCases. The higher binding constants for CP and conventional inhibitors indicate that the CP binding site is different in some way (Table 2). Residues thought to be involved in stabilizing the tetrahedral carbon in the TS are conserved in ROTCase, however, and this suggests that the chemical mechanism of ROTCase also involves the formation of a tetrahedral intermediate. The greatly reduced k_{cat} and increased IE suggest that it is not

just changes to the CP binding domain that are important in ROTCase but that the substitutions in the SMG loop might also be relevant.

Following the conserved SMG motif in the mobile loop of ROTCase is a sequence, -SVSV-, which is unique in known transcarbamoylases. In the crystal structure of apo OTCase from *E. coli* the SMG loop is disordered (*42*), while in the structure of the binary CP complex of the human enzyme the loop is ordered but in an open conformation (*15*). In all structures of complexes which mimic the ternary complex the SMG loop is ordered and in a closed conformation, placing the two substrates sufficiently close for catalysis to occur. The sequence of the ROTCase SMG loop has more hydrophobic residues than the corresponding region in ARGI (Figure 2). Thus it is likely to have different properties to that from ARGI, and this may explain the differences observed in the Michaelis and inhibition constants for the Orn analogues observed for the two enzymes. Furthermore, this difference has potential to affect the k_{cat}. The ternary complex formed on the binding of Orn will involve a ground state ensemble of conformers distinguished by both enzyme and substrate conformations. A fraction of the population of this ensemble is conformers which approximate the structure of the TS and have recently been termed "near-attack conformers" (NAC) (*43*). While the details of this ensemble are unknown for OTCases, it is likely that movements of the so-called SMG loop are involved in the transition to a near-attack conformation. Therefore, prior to the reaction and avoiding high-energy states, the SMG loop in the ternary complex must be present in an ensemble of conformations ranging from at least partially open to approximately closed. The population distribution of the conformers of this ensemble is almost certainly dependent upon the residues of the mobile loop. It is possible, therefore, that these sequence differences identified in this loop reduce the population of NAC for ROTCase and contribute to the much diminished k_{cat} values and poor inhibitory properties of bisubstrate analogues.

Structural analysis of the OTCase/PSorn complex indicated that PSorn is a strong mimic of the TS (*4*). To be effective, TS analogues need to bind the free enzyme in the ground state as well. Resistance to PSorn might occur if the electrostatic topology of the enzyme in apo form, particularly around the CP binding domain, was altered such that PSorn was unable to bind to the free enzyme. Structural information for ROTCase is required to determine whether this is indeed the case.

ACKNOWLEDGMENT

We thank George Bacskay, Department of Chemistry, Sydney University, for advice on the structure of PSorn bound to the OTCase active site, Dave Greenwood and William Laing for critical reading of the manuscript, and Janine Cooney and Dwayne Jensen, HortResearch, for ESMS analysis.

REFERENCES

1. Mitchell, R. E. (1976) Isolation and structure of a chlorosis-inducing toxin of *Pseudomonas phaseolicola*, *Phytochemistry 15*, 1941−1947.
2. Moore, R. E., Neimczura, W. P., Kwok, O. C. H., and Patil, S. S. (1984) Inhibitors of ornithine transcarbamoylase from *Pseudomonas syringae* pv. *phaseolicola*. Revised structure of phaseolotoxin, *Tetrahedron Lett. 25*, 3931−3934.
3. Mitchell, R. E., and Bieleski, R. L. (1977) Involvement of phaseolotoxin in halo blight of beans, *Plant Physiol. 60*, 723−729.
4. Langley, D. B., Templeton, M. D., Fields, B. A., Mitchell, R. E., and Collyer, C. A. (2000) Mechanism of inactivation of ornithine transcarbamoylase by N^{δ}-(*N*′-sulfodiaminophosphinyl)-L-ornithine, a true transition state analogue? Crystal structure and implications for catalytic mechanism, *J. Biol. Chem. 275*, 20012−20019.
5. Goldsmith, J. O., and Kuo, L. C. (1993) Utilization of conformational flexibility in enzyme action-linkage between binding, isomerization, and catalysis, *J. Biol. Chem. 268*, 18481−18484.
6. Miller, A. W., and Kuo, L. C. (1990) Ligand-induced isomerizations of *Escherichia coli* ornithine transcarbamoylase. An ultraviolet difference analysis, *J. Biol. Chem. 265*, 15023−15027.
7. Legrain, C., and Stalon, V. (1976) Ornithine carbamoyltransferase from *Escherichia coli* W: purification, structure and steady-state kinetic analysis, *Eur. J. Biochem. 63*, 289−301.
8. Kuo, L. C., Herzberg, W., and Lipscomb, W. N. (1985) Substrate specificity and protonation state of ornithine transcarbamoylase as determined by pH studies, *Biochemistry 24*, 4754−4761.
9. Kuo, L. C., Miller, A. W., Lee, S., and Cheryl, K. (1988) Site-directed mutagenesis of *Escherichia coli* ornithine transcarbamoylase: role of arginine-57 in substrate binding and catalysis, *Biochemistry 27*, 8823−8832.
10. Goldsmith, J. O., Lee, S., Zambidis, I., and Kuo, L. C. (1991) Control of L-ornithine specificity in *Escherichia coli* ornithine transcarbamoylase. Site-directed mutagenic and pH studies, *J. Biol. Chem. 266*, 18626−18634.
11. Zambidis, I., and Kuo, L. C. (1990) Substrate specificity and protonation state of *Escherichia coli* ornithine transcarbamoylase as determined by pH studies. Binding of carbamoyl phosphate, *J. Biol. Chem. 265*, 2620−2623.
12. Shi, D., Morizono, H., Aoyagi, M., Tuchman, M., and Allewell, N. M. (2000) Human ornithine transcarbamoylase: crystallographic insights into substrate recognition and conformational changes, *Proteins 39*, 271−277.
13. Waldrop, G. L., Urbauer, J. L., and Cleland, W. W. (1992) ^{15}N isotope effects on nonenzymic and aspartate transcarbamoylase catalysed reactions of carbamoyl phosphate, *J. Am. Chem. Soc. 114*, 5941−5945.
14. Parmentier, L. E., Weiss, P. M., O'Leary, M. H., Schachman, H. K., and Cleland, W. W. (1992) ^{13}C and ^{15}N isotope effects as a probe of the chemical mechanism of *Escherichia coli* aspartate transcarbamoylase, *Biochemistry 31*, 6577−6584.
15. Shi, D., Morizono, H., Yu, X., Tong, L., Allewell, N. M., and Tuchman, M. (2001) Human ornithine transcarbamoylase: crystallographic insights into substrate recognition and conformational changes, *Biochem. J. 354*, 501−509.
16. Shi, D., Morizono, H., Ha, Y., Aoyagi, M., Tuchman, M., and Allewell, N. M. (1998) 1.85-Å resolution crystal structure of human ornithine transcarbamoylase complexed with *N*-phosphonacetyl-L-ornithine. Catalytic mechanism and correlation with inherited deficiency, *J. Biol. Chem. 273*, 34247−34254.
17. Massant, J., Wouters, J., and Glansdorff, N. (2003) Refined structure of *Pyrococcus furiosus* ornithine carbamoyltransferase at 1.87 Å, *Acta Crystallogr., Sect. D 59*, 2140−2149.
18. Villeret, V., Clantin, B., Tricot, C., Legrain, C., Roovers, M., Stalon, V., Glansdorff, N., and Van Beeumen, J. (1998) The crystal structure of *Pyrococcus furiosus* ornithine carbamoyltransferase reveals a key role for oligomerization in enzyme stability at extremely high temperatures, *Proc. Natl Acad. Sci. U.S.A. 95*, 2801−2806.
19. Ha, Y., McCann, M. T., Tuchman, M., and Allewell, N. M. (1997) Substrate-induced conformational change in a trimeric ornithine transcarbamoylase, *Proc. Natl Acad. Sci. U.S.A. 94*, 9550−9555.
20. Haworth, N. L., and Bacskay, G. B. (2002) The structure of N^{δ}-(*N*′-sulphodiaminophosphinyl)-L-ornithine and its binding to ornithine transcarbamoylase: a quantum chemical study, *Mol. Simulation 28*, 773−790.
21. Ferguson, A. R., Johnston, J. S., and Mitchell, R. E. (1980) Resistance of *Pseudomonas syringae* pv. *phaseolicola* to its own toxin, phaseolotoxin, *FEMS Microbiol. Lett. 7*, 123−125.
22. Staskawicz, B. J., Panopoulos, N. J., and Hoogenraad, N. J. (1980) Phaseolotoxin-insenstiive ornithine carbamoyltransferase of *Pseudomonas syringae* pv. *phaseolicola*: basis for immunity to phaseolotoxin, *J. Bacteriol. 142*, 720−723.

23. Hatziloukas, E., and Panopoulos, N. J. (1992) Origin, structure, and regulation of *argK*, encoding the phaseolotoxin-resistant ornithine carbamoyltransferase in *Pseudomonas syringae* pv. phaseolicola, and functional expression of *argK* in transgenic tobacco, *J. Bacteriol. 174*, 5895−5909.
24. Mosqueda, G., Van den Broeck, G., Saucedo, O., Bailey, A. M., Alvarez-Moralez, A., and Herrera-Estrella, L. (1990) Isolation and characterisation of the gene from *Pseudomonas syringae* pv. phaseolicola encoding the phaseolotoxin-insensitive ornithine carbamoyltransferase, *Mol. Gen. Genet. 222*, 461−466.
25. Zhang, Y., Rowley, K. B., and Patil, S. S. (1993) Genetic organization of a cluster of genes involved in the production of phaseolotoxin, a toxin produced by *Pseudomonas syringae* pv. phaseolicola, *J. Bacteriol. 175*, 6451−6458.
26. Hatziloukas, E., Panopoulos, N. J., Delis, S., Prosen, D. E., and Schaad, N. W. (1995) An open reading frame in the approximately 28-kb tox-argk gene cluster encodes a polypeptide with homology to fatty acid desaturases, *Gene 166*, 83−87.
27. Zhang, Y. X., and Patil, S. S. (1997) The phtE locus in the phaseolotoxin gene cluster has orfs with homology to genes encoding amino acid transferases, the araC family of transcriptional factors, and fatty acid desaturases, *Mol. Plan− Microbe Interact. 10*, 947−960.
28. Jahn, O., Sauerstein, J., and Reuter, G. (1987) Characterisation of two ornithine carbamoyltransferases from *Pseudomonas syringae* pv. phaseolicola, the producer of phaseolotoxin, *Arch. Microbiol. 147*, 174−178.
29. Templeton, M. D., Sullivan, P. A., and Shepherd, M. G. (1986) Phaseolotoxin-insensitive L-ornithine transcarbamoylase from *Pseudomonas syringae* pv. *phaseolicola*, *Physiol. Mol. Plant Pathol. 29*, 393−403.
30. Rudner, R., Studamire, B., and Jarvis, E. D. (1994) Determinations of restriction fragment length polymorphisms in bacteria using ribosomal RNA genes, *Methods Enzymol. 235*, 184−196.
31. Bencini, D. A., Houghton, J. E., Hoover, T. A., Foltermann, K. F., Wild, J. R., and O'Donovan, G. A. (1983) The DNA sequence of *argI* from *Escherichia coli* K12, *Nucleic Acids Res. 11*, 8509−8518.
32. Brosius, J., and Holy, A. (1984) Regulation of ribosomal RNA promoters with a synthetic lac operator, *Proc. Natl. Acad. Sci. U.S.A. 81*, 6929−6933.
33. Boyde, T. R. C., and Rahmatullah, M. (1980) Optimisation of conditions for the colorimetric determination of citrulline, using diacetyl monoxime, *Anal. Biochem. 107*, 424−431.
34. Templeton, M. D., Sullivan, P. A., and Shepherd, M. G. (1984) The inhibition of ornithine transcarbamoylase from *Escherichia coli* W by phaseolotoxin, *Biochem. J. 224*, 379−388.
35. Ellis, K. J., and Morrison, J. F. (1982) Buffers of constant ionic strength for studying pH-dependent processes, *Methods Enzymol. 87*, 405−426.
36. Cleland, W. W. (1979) Statistical analysis of enzyme kinetic data, *Methods Enzymol. 63*, 103−138.
37. Ramos, F., Stalon, V., Pierard, A., and Wiame, J. M. (1967) The specialization of the two ornithine carbamoyltransferases of *Pseudomonas*, *Biochim. Biophys. Acta 139*, 98−106.
38. Marshall, M., and Cohen, P. P. (1966) A kinetic study of the mechanism of crystalline carbamate kinase, *J. Biol. Chem. 241*, 4197−4208.
39. Parmentier, L. E., O'Leary, M. H., Schachman, H. K., and Cleland, W. W. (1992) ^{13}C isotope effects as a probe of the kinetic mechanism and allosteric properties of *Escherichia coli* aspartate transcarbamoylase, *Biochemistry 31*, 6570−6576.
40. Hoogenraad, N. J., Sutherland, T. M., and Howlett, G. J. (1980) Purification of ornithine transcarbamoylase from rat liver by affinity chromatography with immobilized transition-state analogue, *Anal. Biochem. 101*, 97−102.
41. Parmentier, L. E., and Kristensen, J. S. (1998) Studies on the urea cycle enzyme ornithine transcarbamylase using heavy atom isotope effects, *Biochim. Biophys. Acta 1382*, 333−338.
42. Jin, L., Seaton, B. A., and Head, J. F. (1997) Crystal structure at 2.8 Å resolution of anabolic ornithine transcarbamylase from *Escherichia coli*, *Nat. Struct. Biol. 4*, 622−625.
43. Bruice, T. C. (2002) A view at the millennium: the efficiency of enzymatic catalysis, *Acc. Chem. Res. 35*, 139−148.
44. Cuff, J. A., Clamp, M. E., Siddiqui, A. S., Finlay, M., and Barton, G. J. (1998) Jpred: A Consensus Secondary Structure Prediction Server, *Bioinformatics 14*, 892−893.
45. Penninckx, M., and Gigot, D. (1978) Synthesis and interaction with *Escherichia coli* L-ornithine carbamoyltransferase of two potential transition-state analogues, *FEBS Lett. 88*, 94−96.

BI047432X